

THE MEASURE PRESERVING MARTINGALE SINKHORN ALGORITHM

BENJAMIN JOSEPH^{1*}, GRÉGOIRE LOEPER², AND JAN OBLÓJ³

¹*Mathematical Institute and Christ Church, University of Oxford*

benjamin.joseph@maths.ox.ac.uk

²*BNP Paribas Global Markets*

gregoire.loeper@bnpparibas.com

³*Mathematical Institute and St John's College, University of Oxford*

jan.obloj@maths.ox.ac.uk

ABSTRACT. We contribute to the recent studies of the so-called Bass martingale. Backhoff-Veraguas et al. [2] showed it is the solution to the martingale Benamou-Brenier (mBB) problem, i.e., among all martingales with prescribed initial and terminal distributions it is the one closest to the Brownian motion. We link it with semimartingale optimal transport and deduce an alternative way to derive the dual formulation recently obtained in [3]. We then consider computational methods to compute the Bass martingale. The dual formulation of the transport problem leads to an iterative scheme that mirrors to the celebrated Sinkhorn algorithm for entropic optimal transport. We call it the *measure preserving martingale Sinkhorn* (MPMS) algorithm. We prove that in any dimension, each step of the algorithm improves the value of the dual problem, which implies its convergence. Our MPMS algorithm is equivalent to the fixed-point method of Conze and Henry-Labordère [11], studied in [1], and performs very well on a range of examples, including real market data.

1. INTRODUCTION

We are interested in describing Markov martingales with prescribed marginal distributions. This problem is of fundamental importance in mathematical finance where it corresponds to fitting models to market data. The best known solution, which had a tremendous impact on the financial industry, was given by Dupire [12]. However, this requires knowing marginal distributions at all times requiring elaborate interpolation techniques and suffering from serious numerical stability challenges, see [5]. Instead, we want to build a diffusion process with prescribed marginal distributions at finitely many times. This problem is also intimately related to the classical Skorokhod embedding problem (SEP), see [20], and has recently been re-cast using techniques of optimal transport theory.

In this paper, we focus on the martingale Benamou-Brenier (mBB) problem, i.e., among martingales with prescribed initial and terminal distributions we want to select the one which is closest to Brownian motion, or the constant volatility martingale. This problem was introduced and studied by Backhoff-Veraguas et al. [2] and its solution is given by the so-called Bass martingale, going back to Bass [6] and his solution to the SEP. It is also known as the *stretched Brownian motion* (sBM), and has recently been studied by [3, 4]. Importantly, Conze and Henry-Labordère [11] provided a fixed-point-like iteration scheme for computing the sBM. Its convergence is a topic of a very recent study by Acciaio et al. [1].

Our main contribution is two-fold. First, we link the mBB problem with the literature on semimartingale optimal transport problems. We use the duality results in these works to represent sBM. This mirrors closely the duality results presented in [3] but provides a different point of view. In particular, if we want to generalise the setup to the case where full marginals are not fixed but only constrained (e.g., by a finite number of option prices) this approach is likely to offer more flexibility. Second, we provide a numerical scheme to compute the sBM which mirrors the famous Sinkhorn algorithm used to solve the entropic optimal transport problem, or the Schrödinger problem. Our scheme, dubbed the *measure preserving martingale Sinkhorn* (MPMS) offers a new vantage point on the iterative scheme of [11]. The MPMS iterations we derive are also reminiscent of the

*This research has been supported by BNP Paribas Global Markets and the EPSRC Centre for Doctoral Training in Mathematics of Random Systems: Analysis, Modelling and Simulation (EP/S023925/1).

“back-and-forth method” of [16], which provides a fast iterative method to solve a standard optimal transport problem. Our MPMS scheme displays fast convergence in practice and it offers promising approaches to the higher dimensional setups.

2. MARTINGALE BENAMOU-BRENIER PROBLEM AND ITS DUALITY

We denote $\mathcal{P}_2(\mathbb{R})$ the space of probability measures on \mathbb{R} with a finite second moment. We work with probability measures on \mathbb{R} – this both simplifies the presentation and is the case of interest for applications in mathematical finance. However, our arguments readily generalise to the case of probability measures \mathbb{R}^d . Throughout, we fix $\mu_0, \mu_T \in \mathcal{P}_2(\mathbb{R})$ which admit a density on \mathbb{R} . It will be convenient to identify measures with their densities, so $\mu_0(x)$ will denote the density of μ_0 . It will be clear from the context if we work with a measure or with its density, a function. We also assume that μ_0 and μ_T are in strict convex order, i.e., $\int x d\mu_0 = \int x d\mu_T$ and

$$\int (x - K)^+ \mu_0(dx) < \int (x - K)^+ \mu_T(dx),$$

for all K in the interior of the convex hull of the support of μ_T .¹

We fix a reference volatility value $\bar{\sigma} > 0$ and consider the following martingale Benamou-Brenier (mBB) problem

$$(mBB) \quad \mathbf{MT}_{\mu_0, \mu_T} = \inf_{\substack{M_0 \sim \mu_0, M_T \sim \mu_T \\ M_t = M_0 + \int_0^t \sigma_s dB_s}} \mathbb{E} \left[\int_0^T (\sigma_t - \bar{\sigma})^2 dt \right],$$

where the optimisation is taken over filtered probability spaces with a Brownian motion $(B_t)_{t \geq 0}$. This problem is equivalent to the following problem

$$\mathbf{P}_{\mu_0, \mu_T} = \sup_{\substack{M_0 \sim \mu_0, M_T \sim \mu_T \\ M_t = M_0 + \int_0^t \sigma_s dB_s}} \mathbb{E} \left[\int_0^T |\sigma_t| dt \right] = \sup_{\substack{M_0 \sim \mu_0, M_T \sim \mu_T \\ M_t = M_0 + \int_0^t \sigma_s dB_s}} \mathbb{E} [M_T B_T],$$

in the sense that the two problems share the optimiser and $\mathbf{MT}_{\mu_0, \mu_T} = T\bar{\sigma}^2 + \int x^2 d\mu_T - \int x^2 d\mu_0 - 2\bar{\sigma}\mathbf{P}_{\mu_0, \mu_T}$. These problems were studied in detail by Backhoff-Veraguas et al. [2], with further results relevant for the higher-dimensional setup in the recent works of Backhoff-Veraguas et al. [3] and Backhoff-Veraguas et al. [4]. In particular, [2] show that (mBB) admits a unique optimiser (in distribution) which has a particular representation and is known as the *standard stretched Brownian motion* from μ_0 to μ_T , or the Bass martingale. To describe this process we need to introduce some further notation.

For $\alpha_0 \in \mathcal{P}_2(\mathbb{R})$, we denote $B^\alpha = (B_t^\alpha)_{t \geq 0}$ a Brownian motion with a non-trivial starting law $B_0^\alpha \sim \alpha_0$. We write $B^{\delta_0} = B$, as usual, and for a given B^α let $B_t = B_t^\alpha - B_0^\alpha$ be the associated standard Brownian motion. The heat kernel is denoted

$$\mathbf{R}_t(x) = \frac{1}{\sqrt{2\pi t}} e^{-\frac{x^2}{2t}},$$

and $*$ stands for convolution, so that $B_T^\alpha \sim \alpha_T = \alpha_0 * \mathbf{R}_T$. Finally, $\cdot_\#$ denotes the push-forward operator:

$$F_\# \mu_0 = \mu_T \Leftrightarrow \mu_T = \mu_0 \circ F^{-1} \Leftrightarrow \forall E, \mu_T(E) = \mu_0(F^{-1}(E)).$$

Theorem 2.1 ([2]). *There exists a probability measure $\alpha_0 \in \mathcal{P}_2(\mathbb{R})$ and an increasing function $F : \mathbb{R} \rightarrow \mathbb{R}$ such that $F_\#(\alpha_0 * \mathbf{R}_T) = \mu_T$. The problem (mBB) admits a unique optimiser given by*

$$M_t = \mathbb{E}[F(B_T^\alpha) | \mathcal{F}_t] = F(t, B_t^\alpha),$$

where

$$(1) \quad \begin{aligned} \partial_t F + \frac{1}{2} \partial_{xx} F &= 0, \quad 0 < t < T, x \in \mathbb{R}, \\ F(T, x) &= F(x). \end{aligned}$$

¹This assumption, in the language of MOT, means that there is just one irreducible component.

It follows that the optimiser solves

$$dM_t = F_x(t, B_t^\alpha) dB_t^\alpha = \sigma(t, M_t) dB_t,$$

subject to $M_0 \sim \mu_0$ and $\sigma = F_x \circ F^{-1}$, where the inverse is always taken with respect to the spatial variable.

To gain a different perspective on this process, we note that a class of processes linked to (mBB) was studied via its dual and PDE methods by [15]. More generally, it is a special case of the semimartingale optimal transport studied in [22, 14, 13]. In its general Markovian formulation, one considers

$$(mBB(H)) \quad \mathbf{MT}_{\mu_0, \mu_T}^H := \inf_{\substack{M_0 \sim \mu_0, M_T \sim \mu_T \\ M_t = M_0 + \int_0^t \sigma(s, M_s) dB_s}} \mathbb{E} \left[\int_0^T H(\sigma(t, M_t)^2) dt \right],$$

for a convex function H satisfying suitable regularity assumptions. Then, following the general result stated in [13], we know that duality holds and the minimizer in (mBB(H)) can be obtained by solving the dual problem

$$(2) \quad \mathbf{MT}_{\mu_0, \mu_T}^H = \sup_{\varphi} \left\{ \int_{\mathbb{R}} \varphi(T, x) \mu_T(dx) - \int_{\mathbb{R}} \varphi(0, x) \mu_0(dx) \right\},$$

where the supremum is taken over all super-solutions φ of

$$\partial_t \varphi + H^* \left(\frac{1}{2} \partial_{xx} \varphi \right) \leq 0,$$

with $H^*(p) = \sup_{\sigma \in \mathbb{R}} \{p\sigma - H(\sigma)\}$ the Legendre-Fenchel transform of H . And further, if the supremum is attained by φ then the optimiser is given via

$$\sigma^2(t, x) = H_p^* \left(\frac{1}{2} \partial_{xx} \varphi(t, x) \right).$$

Note that for the cost function

$$(3) \quad H(\beta) = \frac{1}{2} \left(\sqrt{\beta} - \bar{\sigma} \right)^2, \quad \text{we have } H^*(p) = \bar{\sigma}^2 \frac{p}{1 - 2p},$$

and therefore the HJB equation becomes

$$(4) \quad \partial_t \varphi + \frac{1}{2} \frac{\bar{\sigma}^2 \partial_{xx} \varphi}{1 - \partial_{xx} \varphi} = 0,$$

which is well studied in its log-normal form in [18], see also [8, 9, 7]. Assuming that φ is optimal for (2), then the optimal diffusion in (mBB) is given by

$$(5) \quad \sigma = \frac{\bar{\sigma}}{1 - \partial_{xx} \varphi}.$$

Note that for φ to solve the HJB equation, we have that $\partial_{xx} \varphi < 1$. This means that the potential $v = \frac{x^2}{2} - \varphi$ is convex. It further satisfies

$$(6) \quad \partial_t v + \frac{1}{2} \bar{\sigma}^2 \left(1 - \frac{1}{\partial_{xx} v} \right) = 0.$$

Note that the derivative of v , $\xi = \partial_x v$ follows the *linearized* equation

$$(7) \quad \partial_t \xi + \frac{\sigma^2}{2} \partial_{xx} \xi = 0, \quad \text{with } \sigma = \frac{\bar{\sigma}}{\partial_{xx} v} = \frac{\bar{\sigma}}{1 - \partial_{xx} \varphi}.$$

It follows that if we let M^σ solve $dM_t^\sigma = \sigma(t, M_t^\sigma) dB_t$, with σ in (5), then $Z_t := \xi(t, M_t^\sigma)$ is a martingale. Moreover, we have

$$d\langle Z \rangle_t = (\partial_x \xi(t, M_t^\sigma))^2 \sigma(t, M_t^\sigma)^2 dt = \bar{\sigma}^2 dt,$$

and therefore $\frac{1}{\bar{\sigma}} Z$ is a Brownian motion. Observe that the inverse map of ξ is $\partial_y v^*$. If we put $F(t, y) = \partial_y v^*(t, \bar{\sigma} y)$, then $M_t^\sigma = F(t, \frac{1}{\bar{\sigma}} Z_t)$. Further, from (6), we see that the Legendre-Fenchel transform v^* satisfies

$$(8) \quad \partial_t v^* + \frac{1}{2} \bar{\sigma}^2 (\partial_{yy} v^* - 1) = 0,$$

which in turn readily implies that F solves the heat equation, which it has to by the martingale property of M^σ , see (1) above. Note that these functional relations follow simply from φ solving the HJB equation (4). The

marginals are enforced via optimisation over such φ in (2), which gives $M_0^\sigma \sim \mu_0$ and $M_T^\sigma \sim \mu_T$ at the optimiser. However, since F solves the heat equation, we have $F(0, \cdot) = F(T, \cdot) * \mathbf{R}_T$. Comparing with (8) we see that

$$v^*(0, \cdot) = \left(v^*(T, \cdot) - \frac{\bar{\sigma}^2 T}{2} \right) * \mathbf{R}_{T\bar{\sigma}}, \quad \text{and hence}$$

$$v(0, \cdot) = (v^*(T, \bar{\sigma} \cdot) * \mathbf{R}_{T\bar{\sigma}})^* + \frac{\bar{\sigma}^2 T}{2}.$$

We could thus replace the condition that φ solves the HJB equation by the above relation between v , or φ , at times 0 and T . Recall that with H in (3) we have

$$\int_{\mathbb{R}} \varphi(T, x) \mu_T(dx) - \int_{\mathbb{R}} \varphi(0, x) \mu_0(dx) = \mathbf{M} \mathbf{T}_{\mu_0, \mu_T}^H = \frac{1}{2} \mathbf{M} \mathbf{T}_{\mu_0, \mu_T} = \frac{\bar{\sigma}^2 T}{2} + \int_{\mathbb{R}} \frac{x^2}{2} (d\mu_T - d\mu_0) - \bar{\sigma} \mathbf{P}_{\mu_0, \mu_T}.$$

Letting $v(T, \bar{\sigma}^{-1}x) = \psi(x)$, we see that (2) can be equivalently written as

$$(9) \quad \mathbf{P}_{\mu_0, \mu_T} = \inf_{\psi} \left\{ \int_{\mathbb{R}} \psi d\mu_T - \int_{\mathbb{R}} (\psi^* * \mathbf{R}_{T\bar{\sigma}})^* d\mu_0 \right\},$$

which in the special case $\bar{\sigma} = 1$ recovers the duality recently obtained by Backhoff-Veraguas et al. [3].

The densities $\mu(t, x)$ of the marginal distributions M_t^σ satisfy the Fokker-Planck equation

$$\partial_t \mu = \frac{1}{2} \partial_{xx} (\sigma^2 \mu)$$

which implicitly encodes the compatibility condition since both $\mu(0, \cdot) = \mu_0(\cdot)$ and $\mu(T, \cdot) = \mu_T(\cdot)$ are fixed. In particular, the measure α_0 and the function F from Theorem 2.1, are recovered by taking $\bar{\sigma} = 1$ and

$$\alpha_0(\cdot) = \partial_x v(0, \cdot)_{\#} \mu_0 \quad \text{and} \quad F(y) = F(T, y) = \partial_y v^*(T, y).$$

We now explore in more detail these relations and compare with those known for the Sinkhorn system.

3. MEASURE PRESERVING MARTINGALE SINKHORN'S SYSTEM (MPMS)

We fix $\bar{\sigma} = 1 = T$ for simplicity of notation. We start by recalling classical results in entropic optimal transport (EOT).

3.1. Sinkhorn's system. The Schrödinger Problem, a.k.a. EOT problem is stated as finding

$$\inf_{\pi \in \Pi(\mu_0, \mu_1)} \mathbf{KL}(\pi, \mathbb{P}_{\text{ref}}),$$

where \mathbf{KL} is the Kullback-Leibler divergence and we can understand the above either as a problem on the pathspace or equivalently as a problem on \mathbb{R}^2 . In the first case

- $\Pi(\mu_0, \mu_1)$ denotes measures on $C([0, 1]; \mathbb{R})$ with marginals μ_0, μ_1 at times 0, 1 respectively,
- \mathbb{P}_{ref} is the Wiener measure,

and in the second case

- $\Pi(\mu_0, \mu_1)$ denotes probability measure on $\mathbb{R} \times \mathbb{R}$ with given marginals μ_0, μ_1 ,
- \mathbb{P}_{ref} is the standard Gaussian measure on $\mathbb{R} \times \mathbb{R}$.

It is well known that there exist f_0, g_1 such that

(10)	$\mu_0 = (g_1 * \mathbf{R}_1) f_0,$
(11)	$\mu_1 = g_1(\mathbf{R}_1 * f_0),$
(12)	$\mu_t = (g_1 * \mathbf{R}_{1-t})(f_0 * \mathbf{R}_t),$

The system (10)-(11) is known as the *Sinkhorn's system*. It induces an interpolation between μ_0 and μ_1 given by (12). We refer the reader to [17, 19] for great surveys of Entropic Optimal Transport and the Sinkhorn's system. In a nutshell, $\mathbf{R}_1(x, y) f_0(x) g_1(y)$ is the probability measure on $\mathbb{R} \times \mathbb{R}$ that solves the Schrödinger's problem. It induces a probability measure on the canonical space $C([0, 1]; \mathbb{R})$ that is absolutely continuous w.r.t the Wiener measure.

The *Sinkhorn's algorithm* consists in solving iteratively

$$\begin{aligned} \text{Update } f_0 \quad \mu_0 &= (g_1^n * \mathbf{R})f_0^{n+1}, \\ \text{Update } g_1 \quad \mu_1 &= g_1^{n+1}(\mathbf{R} * f_0^{n+1}). \end{aligned}$$

Algorithm 1: Sinkhorn's algorithm

Input: μ_0, μ_1
Output: f_0, g_1
1 Set $g_1^0 = 1$
2 **for** $n = 1$ **to** N_{iter} **do**
3 Solve backward heat equation for g^n $\partial_t g^n + \frac{1}{2} \partial_{xx} g^n = 0, g^n(1) = g_1^n$
4 Update f_0^n such that $f_0^n g^n(0) = \mu_0$
5 Solve forward heat equation for f^n $\partial_t f^n - \frac{1}{2} \partial_{xx} f^n = 0, f^n(0) = f_0^n$
6 Update g_1^{n+1} such that $g_1^{n+1} f^n(1) = \mu_1$
7 **return** f_0, g_1

It can be seen as iterative renormalizations of the kernel \mathbf{R}_1 to have the proper marginals μ_0, μ_1 . It is shown in [21] that this algorithm converges. Moreover, it yields a continuous dynamic interpolation between measures through the system

$$(13) \quad \left\{ \begin{array}{lcl} \partial_t \mu + \nabla_x \cdot (\mu \nabla \varphi) & = & \frac{1}{2} \Delta \mu, \\ \mu(0) & = & \mu_0, \\ \partial_t \varphi + \frac{1}{2} |\nabla \varphi|^2 + \frac{1}{2} \Delta \varphi & = & 0, \\ \varphi(1) & = & \log(g_1). \end{array} \right.$$

The stochastic process associated to this interpolation – with marginals given by μ_t – has unit diffusion and a variable drift.

3.2. MPMS or Sinkhorn for the Bass martingale. Inspired by the above classical results, we propose to re-interpret Theorem 2.1. Our proposed system is naturally in agreement with the fixed point problem addressed in [11], as we explain below. We work again in the setup of Section 2 and $\mu_t = \mu(t, \cdot)$ denote the marginals of the optimiser M^σ of (mBB). We write F_1 for the map F in Theorem 2.1. Theorem 2.1 can be summarised as follows:

$$\begin{aligned} (14) \quad \mu_0 &= (\mathbf{R}_1 * F_1)_\# \alpha_0, \\ (15) \quad \mu_1 &= F_1 \# (\mathbf{R}_1 * \alpha_0), \\ (16) \quad \mu_t &= (\mathbf{R}_{1-t} * F_1)_\# (\mathbf{R}_t * \alpha_0). \end{aligned}$$

This offers a clear analogy to the Sinkhorn system (10)-(12) and suggests an iterative scheme to solve for the Bass martingale. We start with $F_1^0(x) = x$ and

$$\begin{aligned} \text{Update } \alpha_0 \quad \mu_0 &= (F_1^n * \mathbf{R}_1)_\# \alpha_0^{n+1}, \\ \text{Update } F_1 \quad \mu_1 &= (F_1^{n+1})_\# (\mathbf{R}_1 * \alpha_0^{n+1}). \end{aligned}$$

Algorithm 2: Measure Preserving Martingale Sinkhorn's algorithm

Input: μ_0, μ_1
Output: α_0, F_1
1 Set $F_1^0 = Id$
2 **for** $n = 0$ **to** N_{iter} **do**
3 Solve backward heat equation for F^n : $\partial_t F^n + \frac{1}{2} \partial_{xx} F^n = 0, F^n(1) = F_1^n$
4 Update α_0^{n+1} such that $F^n(0)_\# \alpha_0^{n+1} = \mu_0$
5 Solve forward heat equation for α^{n+1} : $\partial_t \alpha^{n+1} - \frac{1}{2} \partial_{xx} \alpha^{n+1} = 0, \alpha^{n+1}(0) = \alpha_0^{n+1}$
6 Update F_1^{n+1} such that $(F_1^{n+1})_\# \alpha^{n+1}(1) = \mu_1$
7 **return** α_0, F_1

It is insightful to comment on the link between MPMS and the fixed-point iteration of Conze and Henry-Labrodère [11]. For a measure ν , let G_ν denote its cumulative distribution function. Recall that for two measures, ν_1 and ν_2 , we have for $h = G_{\nu_1}^{-1} \circ G_{\nu_2}$ that $\nu_1 = h_{\#}\nu_2$. It follows that (14)-(15) can be re-written as

$$\mathbf{R}_1 * F_1 = G_{\mu_0}^{-1} \circ G_{\alpha_0} \quad \text{and} \quad F_1 = G_{\mu_1}^{-1} \circ G_{\mathbf{R}_1 * \alpha_0}.$$

Note also that $G_{\mathbf{R}_1 * \alpha_0} = \mathbf{R}_1 * G_{\alpha_0}$ so that we obtain

$$(17) \quad G_{\alpha_0} = G_{\mu_0} \circ (\mathbf{R}_1 * F_1) = G_{\mu_0} \circ (\mathbf{R}_1 * (G_{\mu_1}^{-1} \circ (\mathbf{R}_1 * G_{\alpha_0})))$$

which is the fixed point relation for G_{α_0} in [11]. In this sense the two algorithms are equivalent, as they have to. Specifically, given a candidate α_0^n , then computing $G_{\mu_1}^{-1} \circ (\mathbf{R}_1 * G_{\alpha_0^n})$ corresponds to lines 5&6 in Algorithm 2, and then applying $G_{\mu_0} \circ (\mathbf{R}_1 * \cdot)$ to the output corresponds to lines 3&4 in Algorithm 2, and yields the updated α_0^{n+1} . One immediate advantage of the representation in Algorithm 2 is that it naturally extends to arbitrary dimensions. Further, we believe this formulation and its analogy to the classical Sinkhorn, will allow for more in depth study of the algorithm and its further relaxations.

We close the chapter by showing that each iteration of MPMS algorithm increases the objective function of the dual problem (2).

Theorem 3.1. *Let $\varphi(t, x)$ solve (4) and $v(t, x) := \frac{x^2}{2} - \varphi(t, x)$ as above. Let $\psi(t, y) := \frac{y^2}{2} + v^*(t, y)$. Let α_0 be defined by $\partial_x \varphi(0, \cdot)_{\#} \alpha_0 = \mu_0$ and $\alpha_T = \gamma_T * \alpha_0$.*

Then any update of $\varphi(T, \cdot)$ (and consequently of $\varphi(\cdot, \cdot)$ through (4)) that increases $\int_{\mathbb{R}} \varphi(T, x) \mu_T(dx) - \int_{\mathbb{R}} \psi(T, x) \alpha_T(dx)$ increases the dual objective function $\int_{\mathbb{R}} \varphi(T, x) \mu_T(dx) - \int_{\mathbb{R}} \varphi(0, x) \mu_0(dx)$. Consequently, the MPMS iterations strictly increase the objective function of the dual problem (2) unless the algorithm has reached a fixed point.

Proof. As shorthand, write $f_t = f(t, \cdot)$ for any function f depending on $(t, x) \in [0, T] \times \mathbb{R}$, and write $d\nu = \nu(dx)$ for a measure ν . Starting from $t = 0$, with distribution μ_0 , let $\tilde{\mu}_t$ be the law of a diffusion process with diffusion given by (5), denoted $\sigma_t(\varphi_t)$. We have that $v_t(x) = \frac{x^2}{2} - \varphi_t(x)$ is convex and at time t , let

$$\alpha_t = \partial_x v_t_{\#} \tilde{\mu}_t.$$

As seen before, α is the distribution of a Brownian motion with initial law α_0 . Let

$$\psi_t(y) = \frac{y^2}{2} + v^*(y),$$

and note ψ_t solves the heat equation :

$$\partial_t \psi_t + \frac{1}{2} \bar{\sigma}^2 \partial_{yy} \psi_t = \bar{\sigma}^2.$$

Therefore,

$$\begin{aligned} \int_{\mathbb{R}} \psi_0 d\alpha_0 + \bar{\sigma}^2 T &= \int_{\mathbb{R}} \psi_T d\alpha_T \\ \operatorname{argsup}_{f(y)-g(x) \leq |y-x|^2/2} \left\{ \int_{\mathbb{R}} f d\tilde{\mu}_t - \int_{\mathbb{R}} g d\alpha_t \right\} &= \{\varphi_t, \psi_t\}. \end{aligned}$$

One could also say that the potential φ_t solves gives the Bass martingale between μ_0 and $\tilde{\mu}_T$. We now have

$$\int_{\mathbb{R}} \varphi_T d\mu_T - \int_{\mathbb{R}} \varphi_0 d\mu_0 = \underbrace{\int_{\mathbb{R}} \varphi_T d\mu_T - \int_{\mathbb{R}} \psi_T d\alpha_T}_{(I)} + \underbrace{\int_{\mathbb{R}} \psi_0 d\alpha_0 - \int_{\mathbb{R}} \varphi_0 d\mu_0}_{(II)} + \bar{\sigma}^2 T.$$

The value (II) is minimal with respect to the pair $\{\psi_0, \varphi_0\}$ for the pair of measures $\{\alpha_0, \mu_0\}$, so any update of φ improves (II). Therefore any improvement of (I) improves the dual objective function. The MPMS algorithm updates $\varphi \mapsto \varphi^{\text{new}}$ such that

$$\partial_x v_T^{\text{new}}_{\#} \mu_T = \alpha_T,$$

or in other words

$$\int_{\mathbb{R}} \varphi_T^{\text{new}} d\mu_T - \int_{\mathbb{R}} \psi_T^{\text{new}} d\alpha_T = \sup_{f(y)-g(x) \leq |y-x|^2/2} \left\{ \int_{\mathbb{R}} f d\mu_T - \int_{\mathbb{R}} g d\alpha_T \right\}.$$

Now assume that $\tilde{\mu}_T \neq \mu_T$, otherwise the algorithm terminates. Note that we do not have to attain the sup in (2) for the result to hold true, we only need to increase $\int_{\mathbb{R}} f d\mu_T - \int_{\mathbb{R}} g d\alpha_T$. Therefore the algorithm increases (I) and when doing so, it updates $\{\varphi_0, \xi_0\}$ in a way that can only increase (II) since the previous pair of dual potentials was optimal (minimal). Therefore

$$\int_{\mathbb{R}} \varphi_T^{\text{new}} d\mu_T - \int_{\mathbb{R}} \varphi_0^{\text{new}} d\mu_0 > \int_{\mathbb{R}} \varphi_T d\mu_T - \int_{\mathbb{R}} \varphi_0 d\mu_0.$$

The algorithm then updates $\alpha_0 \mapsto \alpha_0^{\text{new}} = \partial_x v_0^{\text{new}} \# \mu_0$, and therefore the whole curve α_t , but this has no effect on the dual value. \square

We remark that the result of Theorem 3.1 holds in any dimension. This is seen by considering the d -dimensional version of (mBB) as formulated in [3]. Fix a reference volatility $\bar{\sigma} > 0$, and marginals $\mu_0, \mu_T \in \mathcal{P}_2(\mathbb{R}^d)$ in strict convex order. Then, as in one dimension, we have the equivalent formulation:

$$(mBBd) \quad \mathbf{MT}_{\mu_0, \mu_T} = \inf_{\substack{M_0 \sim \mu_0, M_T \sim \mu_T \\ M_t = M_0 + \int_0^t \sigma_s dB_s}} \mathbb{E} \left[\int_0^T |\sigma_t - \bar{\sigma} \mathbf{I}_d|_{\text{HS}}^2 dt \right],$$

where $|\cdot|_{\text{HS}}$ is the Hilbert-Schmidt norm and \mathbf{I}_d is the $d \times d$ identity matrix. We also have the equivalent formulation of the (mBBd):

$$\mathbf{P}_{\mu_0, \mu_T} = \sup_{\substack{M_0 \sim \mu_0, M_T \sim \mu_T \\ M_t = M_0 + \int_0^t \sigma_s dB_s}} \mathbb{E} \left[\int_0^T \text{tr}(\sigma_t) dt \right],$$

which can be viewed as maximising the covariance of M and Brownian motion. We then consider the more general formulation in a Markovian setting, where we are given a cost function $H : \mathbb{R}^{d \times d} \rightarrow (-\infty, +\infty]$:

$$(mBBd(H)) \quad \mathbf{MT}_{\mu_0, \mu_T}^H := \inf_{\substack{M_0 \sim \mu_0, M_T \sim \mu_T \\ M_t = M_0 + \int_0^t \sigma(s, M_s) dB_s}} \mathbb{E} \left[\int_0^T H(\sigma^\top(t, M_t) \sigma(t, M_t)) dt \right].$$

Once again, applying the general duality result of [13], we arrive at the dual formulation for (mBBd(H)):

$$(18) \quad \mathbf{MT}_{\mu_0, \mu_T}^H = \sup_{\varphi} \left\{ \int_{\mathbb{R}^d} \varphi(T, x) \mu_T(dx) - \int_{\mathbb{R}^d} \varphi(0, x) \mu_0(dx) \right\},$$

where the supremum is taken over all super-solutions φ of

$$(19) \quad \partial_t \varphi + H^* \left(\frac{1}{2} \nabla_x^2 \varphi \right) \leq 0.$$

It is well known that for a positive semidefinite matrix, A , there exists a unique positive semidefinite B such that $B^\top B = A$, which we denote by \sqrt{A} . Therefore, for $\beta \in \mathbb{R}^{d \times d}$, we take the cost function H to be:

$$(20) \quad H(\beta) = \begin{cases} |\sqrt{\beta} - \bar{\sigma} \mathbf{I}_d|_{\text{HS}}^2, & \text{if } \beta \text{ positive semidefinite,} \\ +\infty, & \text{otherwise.} \end{cases}$$

Then, we have that the problems (mBBd(H)) and $\mathbf{P}_{\mu_0, \mu_T}$ are equivalent when H is given by (20), and

$$(21) \quad \int_{\mathbb{R}^d} \varphi(T, x) \mu_T(dx) - \int_{\mathbb{R}^d} \varphi(0, x) \mu_0(dx) = \mathbf{MT}_{\mu_0, \mu_T} = d\bar{\sigma}^2 T + \int_{\mathbb{R}^d} |x|^2 (\mu_T(dx) - \mu_0(dx)) - 2\bar{\sigma} \mathbf{P}_{\mu_0, \mu_T}.$$

Therefore, with φ solving (19), $v = \frac{|x|^2}{2} - \varphi$, and $\psi = v^* + \frac{|y|^2}{2}$, any update of $\varphi(T, \cdot)$ that increases $\int_{\mathbb{R}^d} \varphi(T, x) d\mu_T - \int_{\mathbb{R}^d} \psi(T, x) \alpha_T(dx)$ also increases the value of the dual objective function in (18). The proof of this and that the MPMS iterations increase the value of (18) is identical in d dimensions. For completeness, we now provide a short formal proof of the contraction property in [1, Theorem 1.2], taking advantage of our PDE formulation.

Proposition 3.2 (Contraction Property of [1], Theorem 1.2). *The MPMS algorithm satisfies the contraction property $W^\infty(\alpha_0^{n+1}, \alpha_0^{n+2}) \leq W^\infty(\alpha_0^n, \alpha_0^{n+1})$.*

Proof. The algorithm follows the updates: $\varphi_0^n \mapsto \alpha_0^n \mapsto \alpha_T^n \mapsto \varphi_T^{n+1} \mapsto \varphi_0^{n+1}$. We then have the following sequence of inequalities:

$$\begin{aligned} \text{Update } \alpha_0 &: W^\infty(\alpha_0^n, \alpha_0^{n+1}) \leq \|\partial_x \varphi_0^n - \partial_x \varphi_0^{n+1}\|_{L^\infty}. \\ \text{Heat equation contraction property} &: W^\infty(\alpha_T^n, \alpha_T^{n+1}) \leq W^\infty(\alpha_0^n, \alpha_0^{n+1}). \\ \text{Update } \varphi &: \|\partial_x \varphi_T^{n+1} - \partial_x \varphi_T^{n+2}\|_{L^\infty} = W^\infty(\alpha_T^n, \alpha_T^{n+1}) \\ \text{HJB contraction property} &: \|\partial_x \varphi_0^{n+1} - \partial_x \varphi_0^{n+2}\|_{L^\infty} \leq \|\partial_x \varphi_T^{n+1} - \partial_x \varphi_T^{n+2}\|_{L^\infty} \end{aligned}$$

The first and third point are a direct consequence of the fact that $\partial_x \varphi_{\#} \mu = \alpha$, and for the third point that we are in dimension 1. The second point is a well known fact, that can be easily recovered by considering the case of two Dirac masses evolving through the heat flow. For the fourth point, observe that $\xi = \partial_x \varphi$ solves the parabolic homogeneous PDE

$$(22) \quad \partial_t \xi + \frac{\partial_{xx} \xi}{2(\partial_x \xi)^2} = 0.$$

We claim that $\xi_T \rightarrow \xi_0$ is a contraction in L^∞ . Indeed, this is a general fact for homogeneous nonlinear parabolic equations. Consider the linearized equation of (22). It is a parabolic equation of the form

$$\partial_t u + \mathcal{A}(\xi) \partial_{xx} u + \mathcal{B}(\xi) \partial_x u = 0.$$

It satisfies the maximum principle (at least assuming a growth condition on solutions that we can easily obtain), and therefore $\|u_0\|_{L^\infty(\mathbb{R})} \leq \|u_T\|_{L^\infty(\mathbb{R})}$ with equality only if u is constant. The claim follows easily, and the fourth point of the argument follows.

Finally,

$$W^\infty(\alpha_0^{n+1}, \alpha_0^{n+2}) \leq \|\partial_x \varphi_0^{n+1} - \partial_x \varphi_0^{n+2}\|_{L^\infty} \leq W^\infty(\alpha_0^n, \alpha_0^{n+1}).$$

□

We observe that the only step of the proof that does not work in dimension greater than 1 is the third argument.

4. EXAMPLES AND IMPLEMENTATION OF ALGORITHM 2

We discuss now the practical implementation of Algorithm 2 and present some examples. This algorithm has already been shown to perform very well in [11]. This relies to a large degree on the fact that in one dimension, the transport problem, or the Monge-Ampère equation, can be solved explicitly. This is the observation in (7) which we use for the computation of the pushforwards in Algorithm 2. However, we are also interested in exploring ways to extend this algorithm to other settings, e.g., when the marginal distributions are not entirely fixed or to higher dimensions. One possibility would be to only approximatively solve the transport problem in step 6 in Algorithm 2. This motivated our numerical experiments reported in Appendix A.

In another small departure from the methods in [11], instead of using Gauss-Hermite quadrature to compute the convolutions, we use the observation that α and F solve the forward and backward heat equation respectively to construct an implicit finite difference scheme to compute α_1 and F_0 from α_0 and F_1 respectively. If $0 = t_0 < \dots < t_M = 1$ is a discretisation of the time interval, then we solve the linear systems $A F_{t_k} = F_{t_{k+1}}$ from $F_{t_{k+1}}$ and $\tilde{A} \alpha_{t_k} = \alpha_{t_{k-1}}$. Since $A = \tilde{A}$, we only need to compute $(A^{-1})^M$ once to be able to compute the convolutions. We take a finite interval $[z_{\min}, z_{\max}]$ as our computational domain, and assign the following boundary conditions:

$$\alpha_{t_k}(z_{\min}) = 0, \quad \alpha_{t_k}(z_{\max}) = 1, \quad F_{t_k}(z_{\min}) = z_{\min}, \quad F_{t_k}(z_{\max}) = z_{\max}, \quad \text{for } k = 1, \dots, M.$$

In all of our examples, we measure the error by $\frac{1}{N} \sum_{k=1}^N \left(G_{\mu_0}^{-1}(y_k) - G_{(F_1^n * \mathbf{R}_1)_{\#} \alpha_0^n}^{-1}(y_k) \right)^2$ where $0 = y_1 < \dots < y_N = 1$ is a uniform discretisation of $[0, 1]$, so that we are minimising in mean square the horizontal distance between the CDFs. We start with a mixed Gaussian example with our marginals given by

$$(23) \quad \mu_0 = \mathcal{N}(0, 0.5), \quad \mu_1 = \frac{1}{4} \mathcal{N}(-1, 0.25) + \frac{1}{2} \mathcal{N}(0, 0.5) + \frac{1}{4} \mathcal{N}(1, 0.25).$$

We discretised the interval $[-4, 4]$ into 1000 spatial gridpoints, and the time interval $[0, 1]$ into 50 gridpoints. We ran Algorithm 2 until an error of 1×10^{-10} was reached, which took 9 iterations – equivalent to 0.067 seconds².

²All computational times reported are for a laptop with 16GB RAM and i5-10310U CPU @ 1.70GHz.

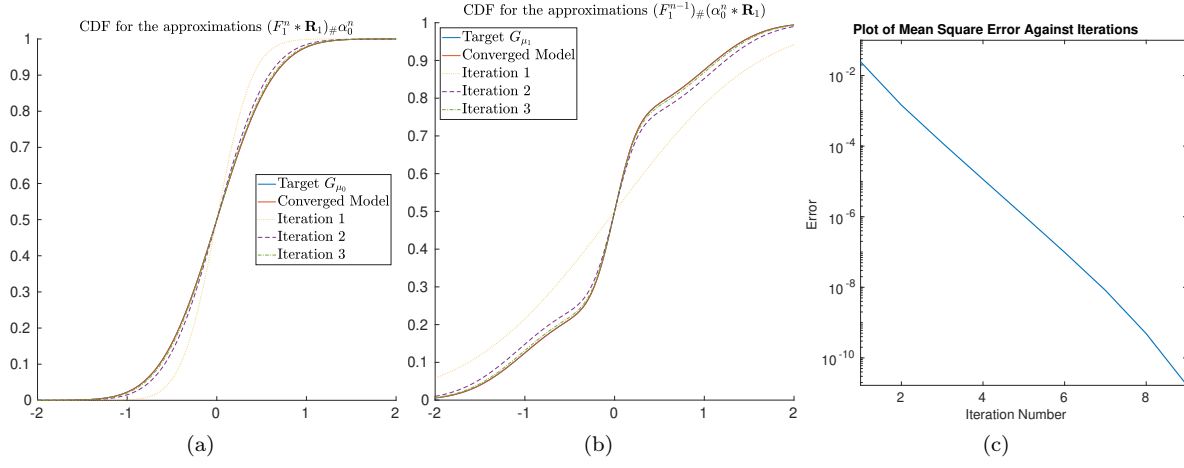


FIGURE 1. Example (23). (a) Plots of CDF for the approximations of μ_0 after various iterations along with the target CDF, (b) Plots of CDF for the approximations of μ_1 after various iterations along with the target CDF, (c) Plot of mean square error as a function of iteration.

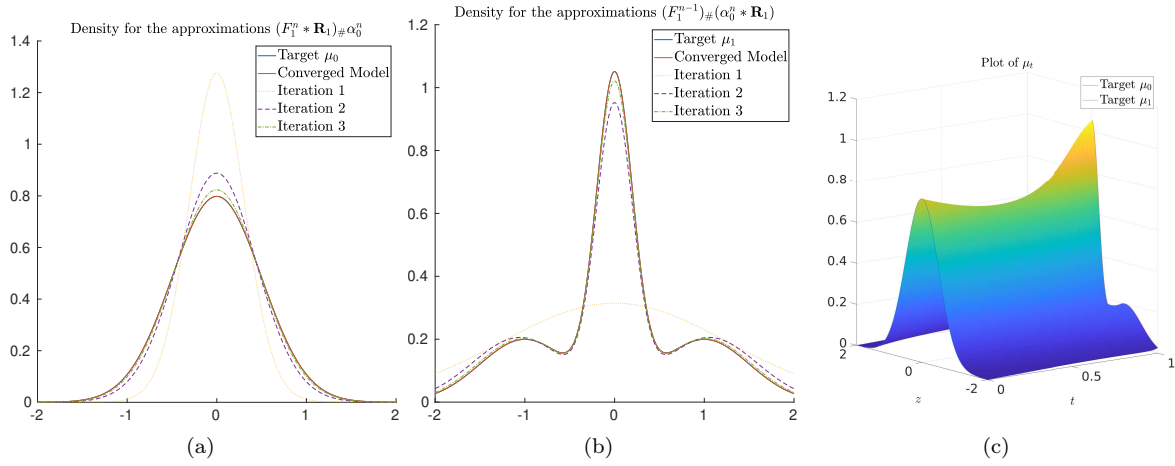


FIGURE 2. Example (23). (a) Plots of the density for the approximations of μ_0 along with the target density, (b) Plots of the density for the approximations of μ_1 along with the target density (c) Plot of converged density martingale interpolation viewed from $t = 0$.

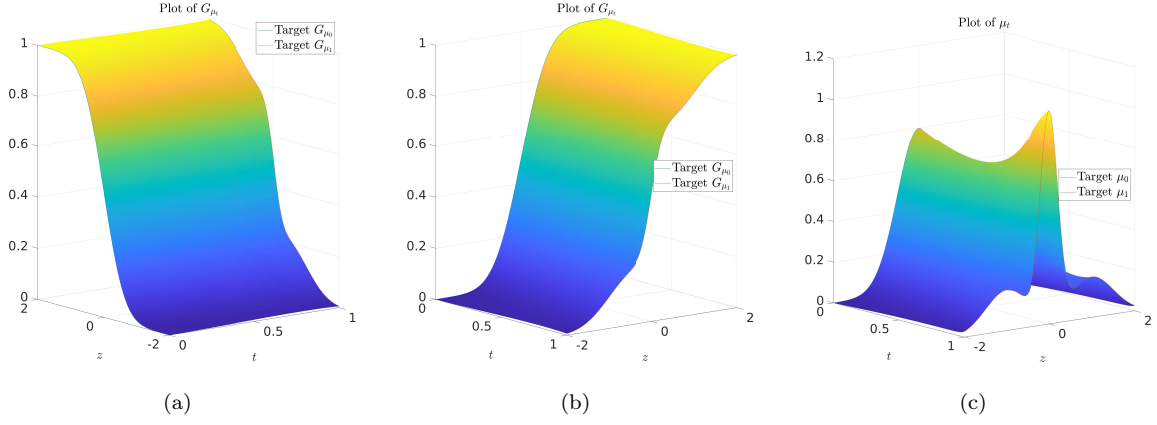


FIGURE 3. Example (23). (a) Plot of CDF martingale interpolation viewed from $t = 0$, (b) Plot of CDF martingale interpolation viewed from $t = 1$, (c) Plot of density martingale interpolation viewed from $t = 1$.

We next try a lognormal example, where the prescribed marginals are given by

$$(24) \quad \mu_0 = \text{Lognormal}\left(r - \frac{1}{2}\sigma_0^2, \sigma_0\right), \quad \mu_1 = \text{Lognormal}(2r - \sigma_1^2, \sigma_1).$$

Where $r = 0.05$, $\sigma_0 = 0.2$, and $\sigma_1 = 0.4$, so that this resembles a Geometric Brownian motion with different volatilities. We took the same time discretisation as in the weighted Gaussian example, but our spatial interval was given instead by $[0.25, 7]$, which was discretised into 1000 gridpoints. We ran Algorithm 2 until an error of 1×10^{-8} was attained, which took 57 iterations – equivalent to 0.35 seconds.

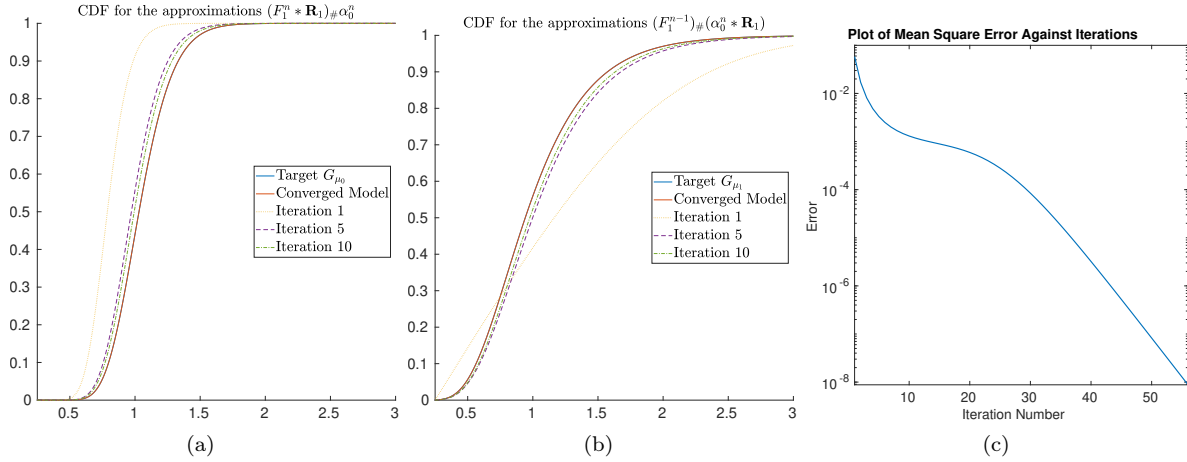


FIGURE 4. Example (24). (a) Plots of CDF for the approximations of μ_0 after various iterations along with the target CDF, (b) Plots of CDF for the approximations of μ_1 after various iterations along with the target CDF, (c) Plot of mean square error as a function of iteration.

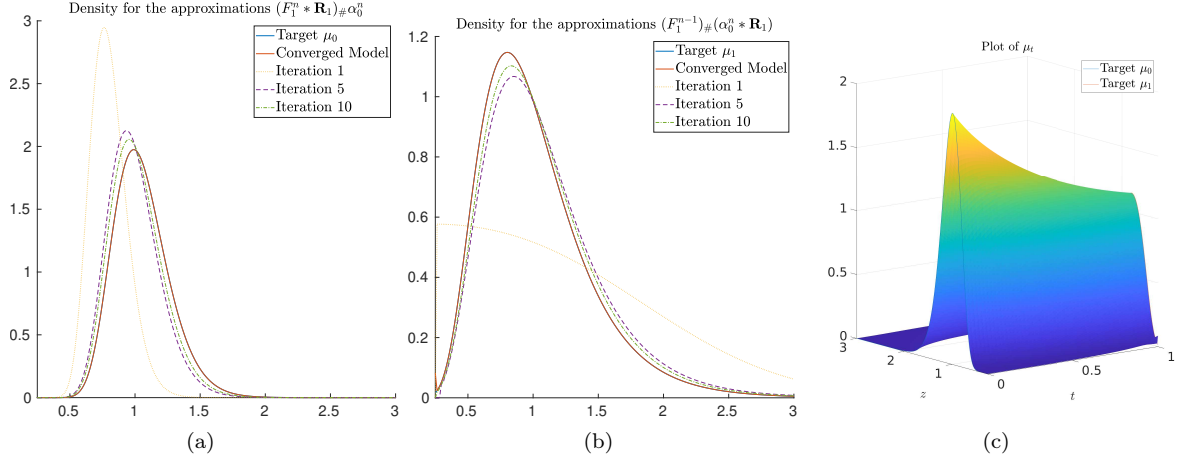


FIGURE 5. Example (24). (a) Plots of the density for the approximations of μ_0 along with the target density, (b) Plots of the density for the approximations of μ_1 along with the target density (c) Plot of converged density martingale interpolation viewed from $t = 0$.

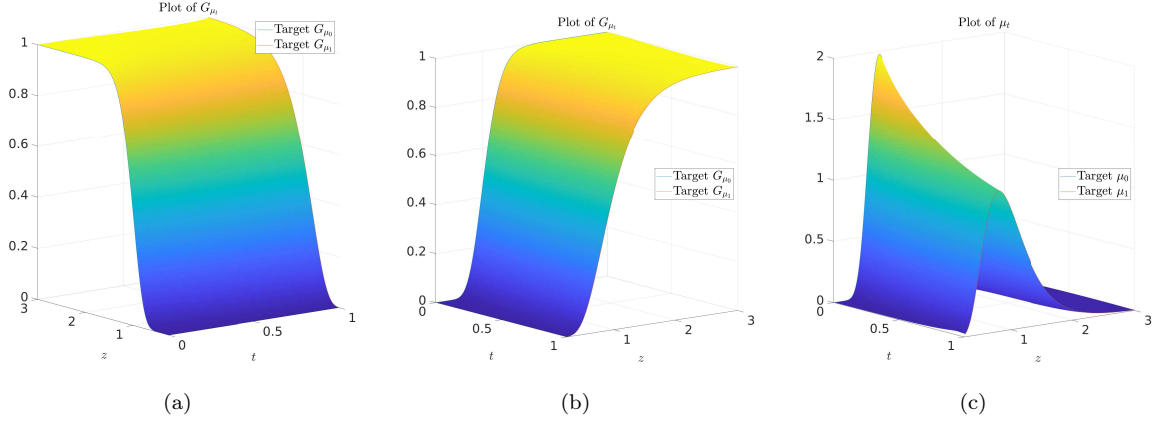


FIGURE 6. Example (24). (a) Plot of CDF martingale interpolation viewed from $t = 0$, (b) Plot of CDF martingale interpolation viewed from $t = 1$, (c) Plot of density martingale interpolation viewed from $t = 1$.

Finally, we benchmark the MPM-Sinkhorn iterations using the Breeden-Litzenberger formula of [10]. Let $C(T, K)$ be the price of a European call option on an underlying with maturity $T > 0$ and strike $K > 0$, then the density of the underlying at time T is given by $\mu_T(K) = \frac{\partial^2 C(T, K)}{\partial K^2}$. In order to compute the second derivative of the call option price, we interpolated the strikes and prices with a spline. Owing to numerical instabilities in computing the second derivative, we also applied a smoothing formula to generate more reasonable densities. We obtained³ SPX call option data with maturities at 20/12/2024 and 19/12/2025, which we denote T_0 and T_1 respectively. We discretised $[T_0, T_1]$ into 50 gridpoints, and took the spatial interval of $[1200, 8000]$ and discretised it into 1000 gridpoints. We then rescaled the domain and the densities by 1000. Since the CDFs are numerically computed from interpolated options data, we took a higher tolerance at 5×10^{-6} , and obtained convergence in 28 iterations which took 0.18 seconds.

³Data obtained from https://www.cboe.com/delayed_quotes/spx on 08/08/2023.

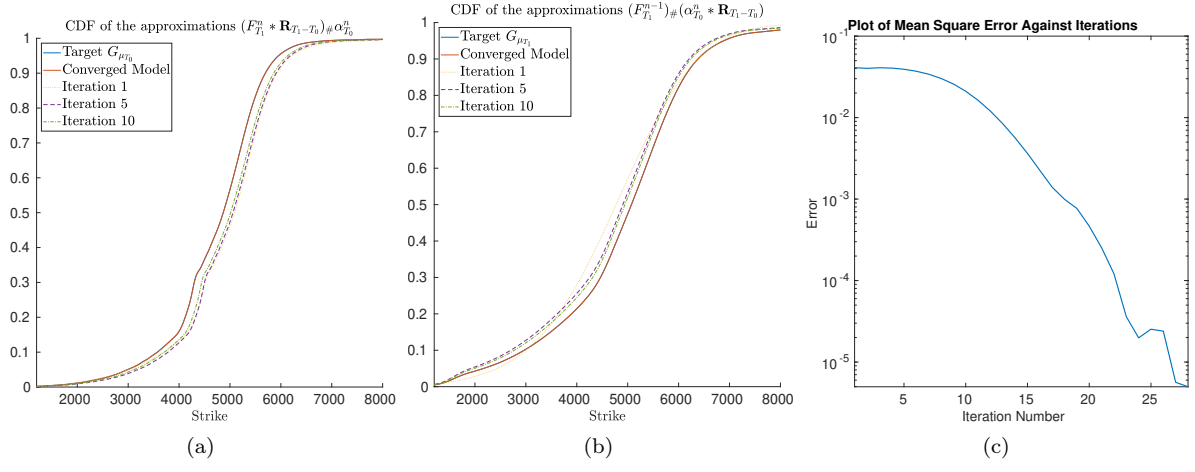


FIGURE 7. SPX market data example. (a) Plots of CDF for the approximations of μ_{T_0} after various iterations along with the target CDF, (b) Plots of CDF for the approximations of μ_{T_1} after various iterations along with the target CDF, (c) Plot of mean square error as a function of iteration.

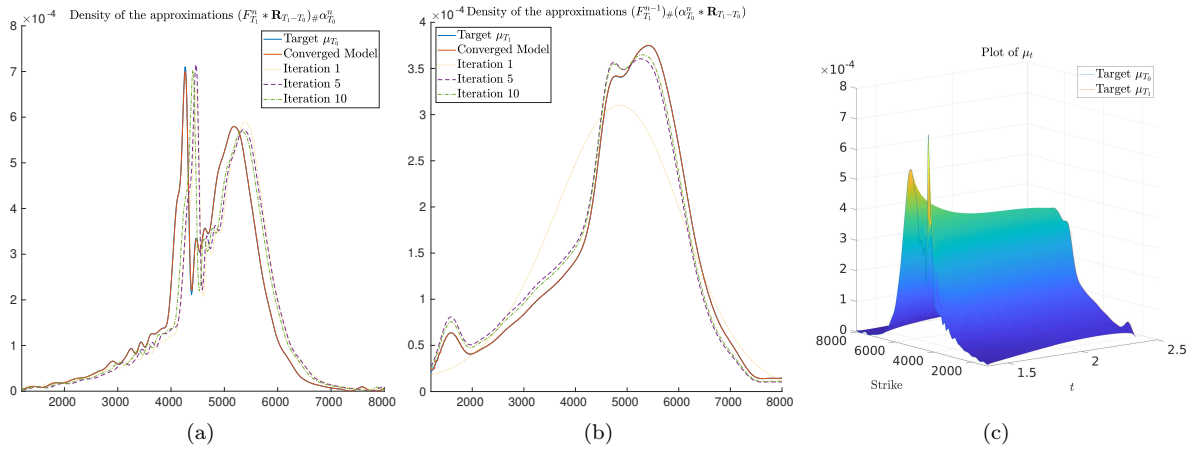


FIGURE 8. SPX market data example. (a) Plots of the density for the approximations of μ_{T_0} along with the target density, (b) Plots of the density for the approximations of μ_{T_1} along with the target density (c) Plot of converged density martingale interpolation viewed from $t = T_0$.

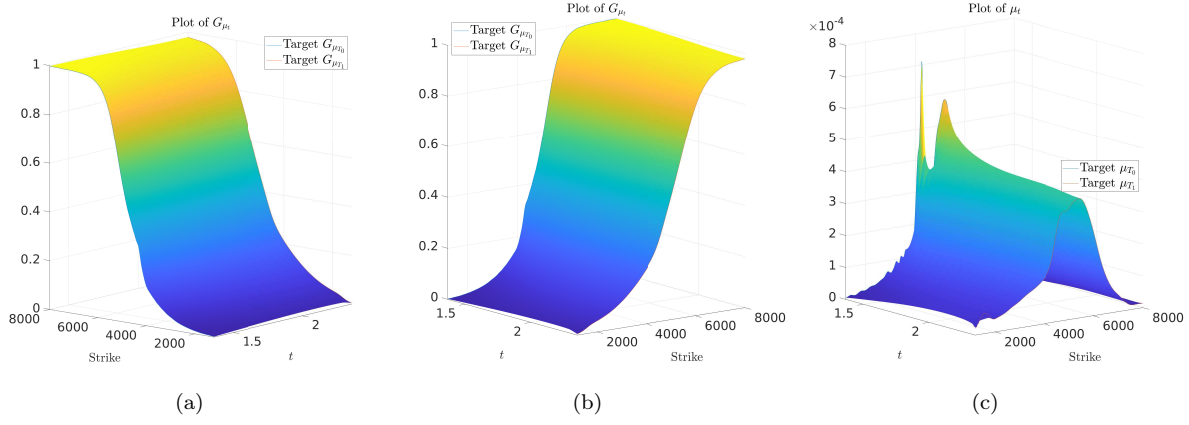


FIGURE 9. SPX market data example. (a) Plot of CDF martingale interpolation viewed from $t = T_0$, (b) Plot of CDF martingale interpolation viewed from $t = T_1$, (c) Plot of density martingale interpolation viewed from $t = T_1$.

APPENDIX A. AN ALTERNATIVE IMPLEMENTATION WITH AN APPROXIMATE TRANSPORT SOLUTION

We now provide an alternative implementation of Algorithm 2, where we deal with the densities directly. We write $f = F'$ and f^n for the derivative of F^n . In the algorithm, we have to twice solve the transport relation $\nu_1 = h_{\#}\nu_2$ with two of ν_1, ν_2, h given. For a given $\nu_1 \in \mathcal{P}_2(\mathbb{R})$ and a (differentiable strictly increasing) h , a change of variables gives $\nu_2(y) = \nu_1(h(y))h'(y)$. In particular, line 4 in Algorithm 2 reads $\alpha_0^n(y) = \mu_0(F^n(0, y))f^n(0, y)$. On the other hand, for a given $\nu_1, \nu_2 \in \mathcal{P}_2(\mathbb{R})$, we have $h = G_{\nu_1}^{-1} \circ G_{\nu_2}$. We thus consider the equivalent implicit equation for h : $\nu_2(y) = \nu_1(h(y))h'(y)$ and use the previous estimate for $h(y)$ to solve for $h'(y)$ and integrate numerically. In summary, our alternative implementation for Algorithm 2 reads as follows:

Algorithm 3: MPMS: density implementation

<p>1 Set $F_1^0 = Id, f_1^0 = 1$;</p> <p>2 for $n = 0$ to N_{iter} do</p> <p>3 Compute α_0^{n+1}:</p> <p>4 Compute f_1^{n+1} using F_1^n and α_0^n:</p> <p>5 Compute $F_1^{n+1}(x)$:</p> <p>6 return α_0, F_1, f_1</p>	$\alpha_0^{n+1}(x) = \mu_0((F_1^n * \mathbf{R}_1)(x))(f_1^n * \mathbf{R}_1)(x);$ $f_1^{n+1}(x) = \frac{(\alpha_0^n * \mathbf{R}_1)(x)}{\mu_1(F_1^n(x))};$ $F_1^{n+1}(x) = \int_{-\infty}^x f_1^{n+1}(y)dy.$
---	---

In practice, the above has to be implemented on a discrete grid and has to address the issue of division by zero. We let $x_i, i = 1, \dots, N$ be a discretisation of the desired interval to apply the convolution on and let $y_i = \frac{1}{m}(x_i - c)$ be a rescaling of the discretisation such that most of the mass of μ_1 is contained in $[y_1, y_N]$, i.e., $\int_{y_1}^{y_N} \mu_1 dy \approx 1$. We also replace f_1^{n+1} with $f_1^{n+1} \wedge C$ to avoid issues around division in line 4 above; in the region of the domain where both $\alpha_0^n * \mathbf{R}_1$ and $\mu_1(F_1^n)$ are close to zero, we set $f_1^{n+1} = 0$. Let `conv` denote a numerical implementation of the convolution and $\text{conv}(\cdot)_k$ denote the k^{th} element of the vector returned by `conv`. Then, the above algorithm can be implemented as follows:

$$F_1^0(x_k) = x_k, \quad f_1^0(x_k) = 1, \quad k = 1, \dots, N;$$

(25)

$$\begin{cases} F_1^n * \mathbf{R}_1(x_k) &= \text{conv}(mF_1^n + c, \mathbf{R}_1)_k, \\ f_1^n * \mathbf{R}_1(x_k) &= \text{conv}(mf_1^n + c, \mathbf{R}_1)_k, \\ \alpha_0^n(y_k) &= \frac{1}{m}(f_1^n * \mathbf{R}_1(x_k) - c * \mathbf{R}_1(x_k)) \mu_0\left(\frac{1}{m}(F_1^n * \mathbf{R}_1(x_k) - c * \mathbf{R}_1(x_k))\right), \end{cases}$$

(26)

$$\begin{cases} \alpha_0^n * \mathbf{R}_1(x_k) &= \text{conv}(m\alpha_0^n + c, \mathbf{R}_1)_k \\ f_1^n(y_k) &= \begin{cases} \left(\frac{1}{m} (\alpha_0^n * \mathbf{R}_1(x_k) - c * \mathbf{R}_1(x_k)) / \mu_1(F_1^n(y_k)) \right) \wedge C, & \text{if } \alpha_0^n * \mathbf{R}_1(x_k) - c * \mathbf{R}_1(x_k) \neq 0 \neq \mu_1(F_1^n(y_k)), \\ 0, & \text{if } \alpha_0^n * \mathbf{R}_1(x_k) - c * \mathbf{R}_1(x_k) = 0 = \mu_1(F_1^n(y_k)), \end{cases} \\ F_1^{n+1}(y_k) &= F_1^n(y_1) + \int_{y_1}^{y_k} f_1^n(y) dy, \quad k = 1, \dots, N. \end{cases}$$

Since we only approximately solve $\mu_1 = F_{\#}(\alpha_0 * \mathbf{R}_1)$, we must control the error at both $t = 0$ and $t = 1$. We therefore take the maximum of the mean square error of the inverse CDFs at $t = 0$ and $t = 1$. Since the CDFs and their inverse must both be numerically computed, we had to take lower tolerances in this implementation.

We start with the weighted Gaussian with marginals given by (23). We discretised the interval $[-4, 4]$ into 1000 spatial gridpoints, and applied the iterations (25)-(26) until a mean square error of 1×10^{-5} was achieved. The upper bound in (26) was taken to be $C = 1.5$. This took a total of 71 iterations which was equivalent to 0.27 seconds.

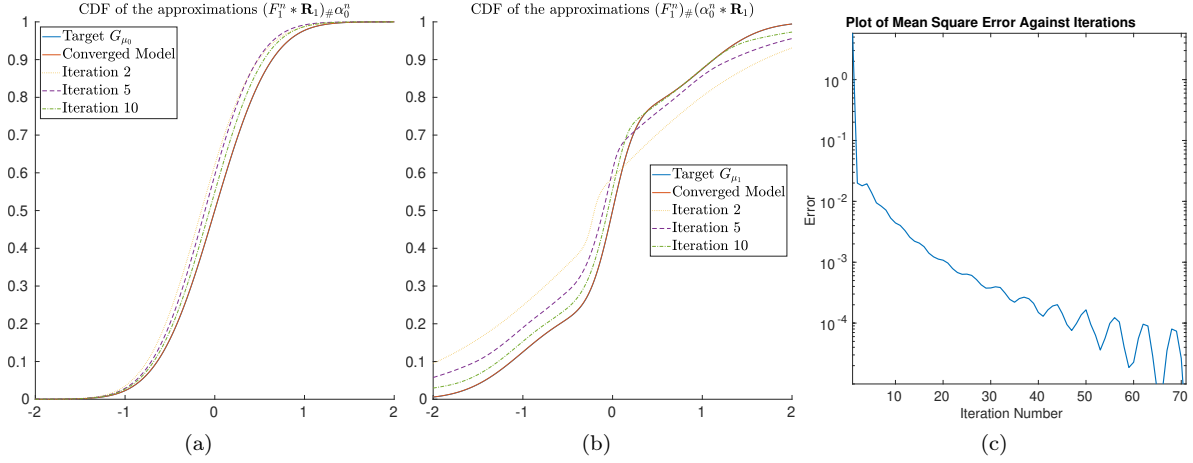


FIGURE 10. Example (23). (a) Plots of CDF for the approximations of μ_0 after various iterations along with the target CDF, (b) Plots of CDF for the approximations of μ_1 after various iterations along with the target CDF, (c) Plot of mean square error in μ_0 as a function of iteration.

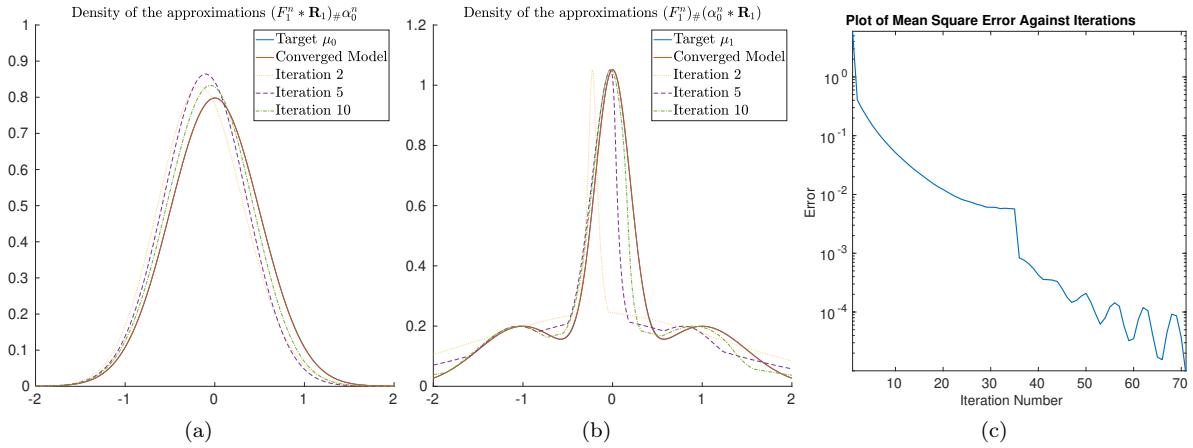


FIGURE 11. Example (23). (a) Plots of the density for the approximations of μ_0 along with the target density, (b) Plots of the density for the approximations of μ_1 along with the target density (c) Plot of mean square error in μ_1 as a function of iteration.

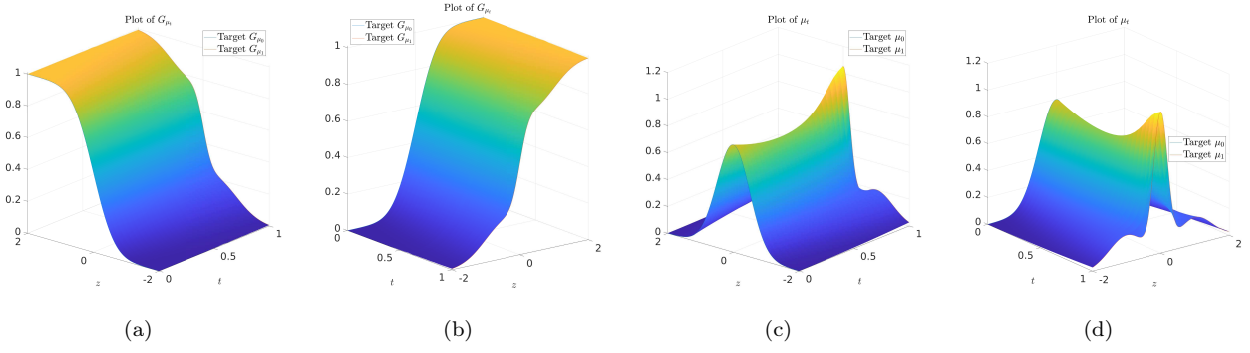


FIGURE 12. Example (23). (a) Plot of CDF martingale interpolation viewed from $t = 0$, (b) Plot of CDF martingale interpolation viewed from $t = 1$, (c) Plot of density martingale interpolation viewed from $t = 0$, (d) Plot of density martingale interpolation viewed from $t = 1$.

We next try repeat the lognormal example with marginals given by (24). We used the domain $[-3.9, 4.1]$ and mapped it onto $[0.2, 5]$ for μ_0 and $[0.25, 10]$ for μ_1 each with 1000 gridpoints. As before, the iterations (25)-(26) were repeated until an error of 1×10^{-6} was achieved, this time the upper bound in (26) was set to $C = 2.4$. This took 47 iterations, which was equivalent to 0.19 seconds.

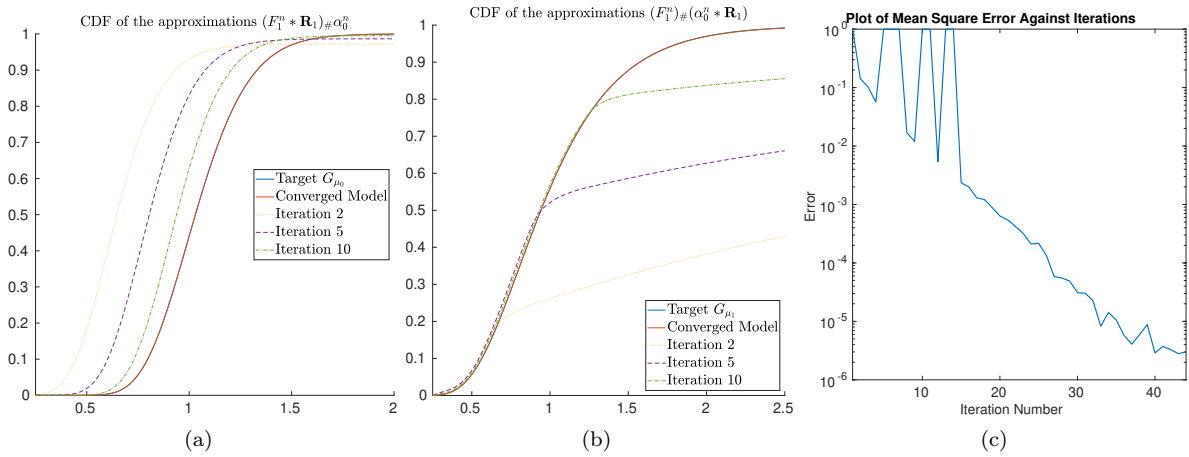


FIGURE 13. Example (24). (a) Plots of CDF for the approximations of μ_0 after various iterations along with the target CDF, (b) Plots of CDF for the approximations of μ_1 after various iterations along with the target CDF, (c) Plot of mean square error in μ_0 as a function of iteration.

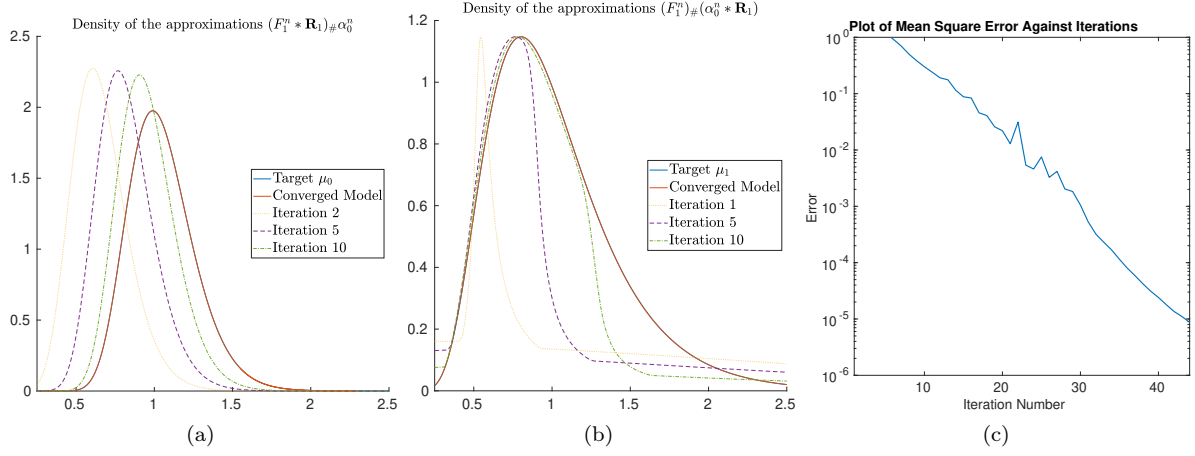


FIGURE 14. Example (24). (a) Plots of the density for the approximations of μ_0 along with the target density, (b) Plots of the density for the approximations of μ_1 along with the target density (c) Plot of mean square error in μ_1 as a function of iteration.

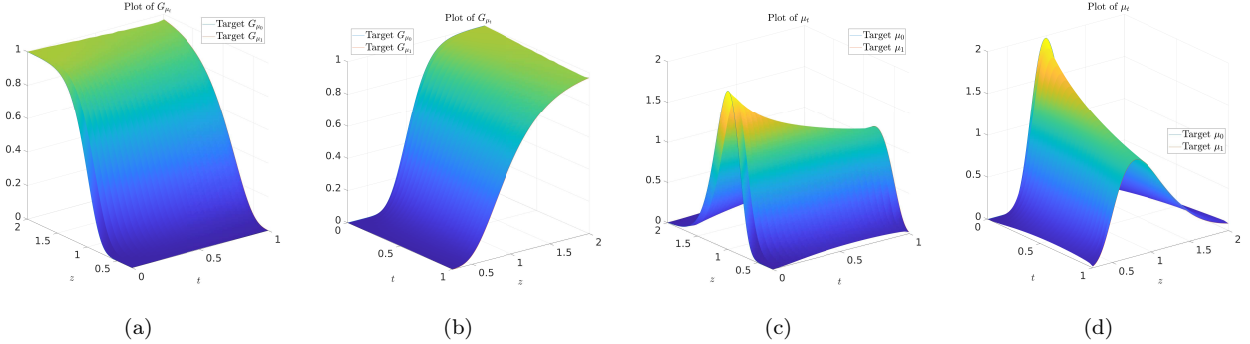


FIGURE 15. Example (24). (a) Plot of CDF martingale interpolation viewed from $t = 0$, (b) Plot of CDF martingale interpolation viewed from $t = 1$, (c) Plot of density martingale interpolation viewed from $t = 0$, (d) Plot of density martingale interpolation viewed from $t = 1$.

Finally, we repeat the Breeden-Litzenberger example using Algorithm 3. We used the domain $[-10, 10]$, and mapped it onto $[1200, 8000]$ for μ_{T_0} and μ_{T_1} . Due to numerical issues in computing the model inverse CDFs, we used the mean square difference between CDFs as the error. We iterated (25)-(26) until we an error of 5×10^{-5} was attained, and took the upper bound in (26) to be $C = 2.7$. This took a total of 57 iterations, for a total computational time of 0.18 seconds. If we wanted to extend the model onto the interval $[0, T_0]$, since we have no marginal constraints, we can use the fact that F solves the heat equation, so that for $t \in [0, T_0]$, we have $F(t, \cdot) = \mathbf{R}_{T_0-t} * F(T_0, \cdot)$.

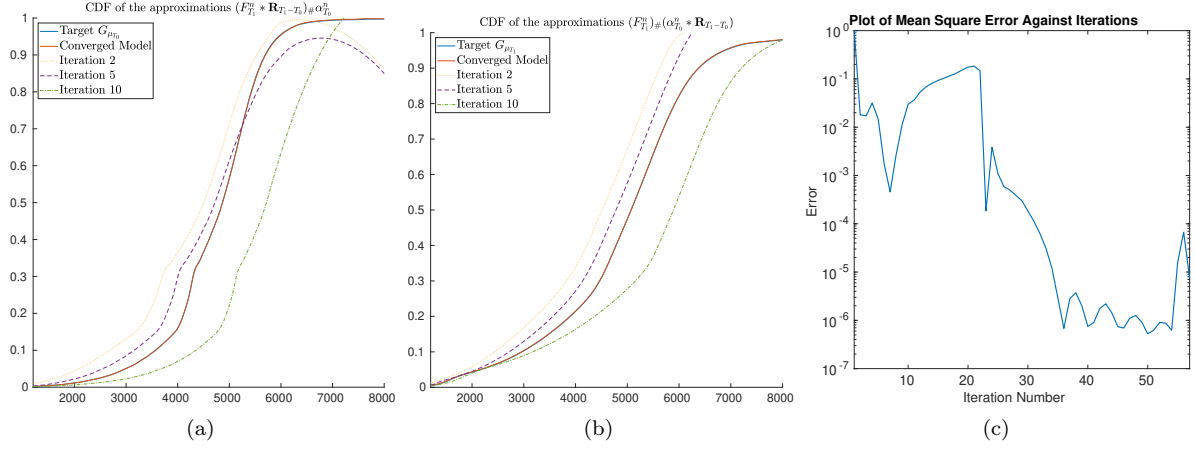


FIGURE 16. SPX market data example. (a) Plots of CDF for the approximations of μ_{T_0} after various iterations along with the target CDF, (b) Plots of CDF for the approximations of μ_{T_1} after various iterations along with the target CDF, (c) Plot of mean square error in μ_{T_0} as a function of iteration.

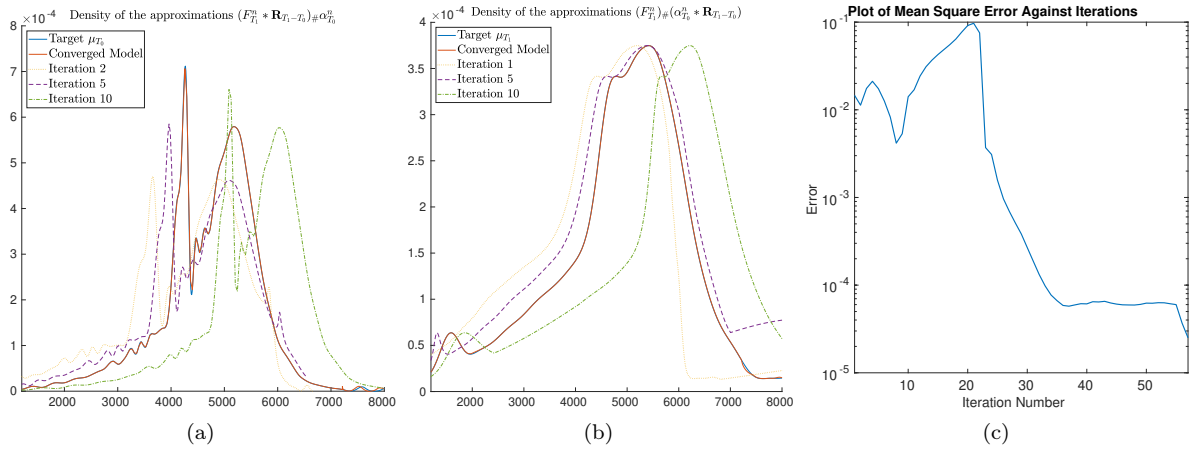


FIGURE 17. SPX market data example. (a) Plots of the density for the approximations of μ_{T_0} along with the target density, (b) Plots of the density for the approximations of μ_{T_1} along with the target density (c) Plot of mean square error in μ_{T_1} as a function of iteration.

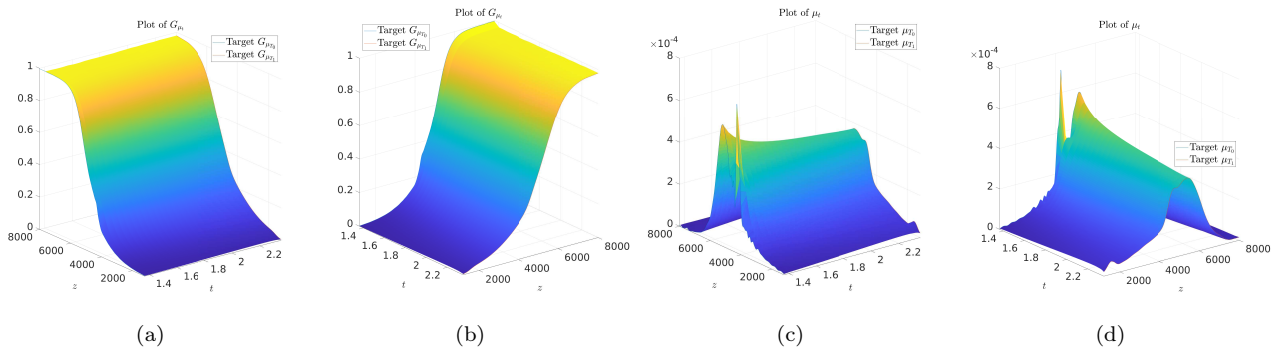


FIGURE 18. SPX market data example. (a) Plot of CDF martingale interpolation viewed from $t = T_0$, (b) Plot of CDF martingale interpolation viewed from $t = T_1$, (c) Plot of density martingale interpolation viewed from $t = T_0$, (d) Plot of density martingale interpolation viewed from $t = T_1$.

REFERENCES

- [1] Beatrice Acciaio, Antonio Marini, and Gudmund Pammer. Calibration of the bass local volatility model. *arXiv preprint arXiv:2311.14567*, 2023.
- [2] Julio Backhoff-Veraguas, Mathias Beiglböck, Martin Huesmann, and Sigrid Källblad. Martingale Benamou–Brenier: a probabilistic perspective. *Ann. Probab.*, 48(5):2258–2289, 2020.
- [3] Julio Backhoff-Veraguas, Mathias Beiglböck, Walter Schachermayer, and Bertram Tschiderer. The Structure of martingale Benamou-Brenier in \mathbb{R}^d . *arXiv preprint arXiv:2306.11019*, 2023.
- [4] Julio Backhoff-Veraguas, Walter Schachermayer, and Bertram Tschiderer. The bass functional of martingale transport. *arXiv preprint arXiv:2306.11019*, 2023.
- [5] Alan Bain, Matthieu Mariapragassam, and Christoph Reisinger. Calibration of local-stochastic and path-dependent volatility models to vanilla and no-touch options. *Journal of Computational Finance*, 24(4), 2021.
- [6] Richard F Bass. Skorokhod imbedding via stochastic integrals. *Séminaire de probabilités de Strasbourg*, 17:221–224, 1983.
- [7] Bruno Bouchard, Grégoire Loeper, Halil Mete Soner, and Chao Zhou. Second-order stochastic target problems with generalized market impact. *SIAM J. Control Optim.*, 57(6):4125–4149, 2019.
- [8] Bruno Bouchard, Grégoire Loeper, and Yiyi Zou. Almost-sure hedging with permanent price impact. *Finance Stoch.*, 20(3):741–771, 2016.
- [9] Bruno Bouchard, Grégoire Loeper, and Yiyi Zou. Hedging of covered options with linear market impact and gamma constraint. *SIAM J. Control Optim.*, 55(5):3319–3348, 2017.
- [10] Douglas T Breeden and Robert H Litzenberger. Prices of state-contingent claims implicit in option prices. *Journal of business*, pages 621–651, 1978.
- [11] Antoine Conze and Pierre Henry-Labordère. Bass construction with multi-marginals: Lightspeed computation in a new local volatility model. *Available at SSRN 3853085*, 2021.
- [12] B. Dupire. Pricing with a smile. *RISK*, January:18–20, 1994.
- [13] Ivan Guo and Grégoire Loeper. Path dependent optimal transport and model calibration on exotic derivatives. *Ann. Appl. Probab.*, 31(3):1232–1263, 2021.
- [14] Ivan Guo, Grégoire Loeper, and Shiyi Wang. Local volatility calibration by optimal transport. In *2017 MATRIX annals*, volume 2 of *MATRIX Book Ser.*, pages 51–64. Springer, Cham, 2019.
- [15] Martin Huesmann and Dario Trevisan. A benamou–brenier formulation of martingale optimal transport. *Bernoulli*, 25(4A):2729–2757, 2019.
- [16] Matt Jacobs and Flavien Léger. A fast approach to optimal transport: The back-and-forth method. *Numerische Mathematik*, 146(3):513–544, 2020.
- [17] Christian Léonard. A survey of the Schrödinger problem and some of its connections with optimal transport. *Discrete Contin. Dyn. Syst.*, 34(4):1533–1574, 2014.
- [18] Gregoire Loeper. Option pricing with linear market impact and nonlinear Black-Scholes equations. *Ann. Appl. Probab.*, 28(5):2664–2726, 2018.
- [19] Marcel Nutz. Introduction to entropic optimal transport. 2022.
- [20] Jan Oblój. The Skorokhod embedding problem and its offspring. *Probability Surveys*, 1:321–392, 2004.
- [21] Richard Sinkhorn. A relationship between arbitrary positive matrices and doubly stochastic matrices. *Ann. Math. Statist.*, 35:876–879, 1964.
- [22] Xiaolu Tan and Nizar Touzi. Optimal transportation under controlled stochastic dynamics. *Ann. Probab.*, 41(5):3201–3240, 2013.